

# Analysis of CH<sub>2</sub>OxOH as marker for fuel-rich air to pure oxy-fuel flames under higher preheat temperature and elevated pressure

M. Sentko<sup>1\*</sup>, P. Habisreuther<sup>1</sup>, G. Vourliotakis<sup>2</sup>, C. Keramiotis<sup>2</sup>, B. Stelzner<sup>1</sup>, M. Founti<sup>2</sup>, D. Trimis<sup>1</sup>

<sup>1</sup>Engler-Bunte-Institute Combustion Technology, Karlsruhe Institute of Technology, Karlsruhe, Germany

<sup>2</sup>Lab. of Heterogeneous Mixtures and Combustion Systems, School of Mechanical Engineering, NTU of Athens, Greece

## Abstract

The scope of the present work is a numerical and experimental investigation about the range of validity in terms of applicability of CH<sub>2</sub>OxOH as a marker for the heat release rate (HRR) for fuel-rich air to pure oxy-fuel flames including preheating and elevated pressure. Therefore, laminar, freely propagating 1d CH<sub>4</sub> flames were calculated, where oxygen content in the oxidizer (from air to pure oxy-fuel combustion), inlet temperature and pressure were varied for a wide range of the equivalence ratios. The preheat temperature and pressure were parametrically changed from 300 K to 573 K and 1 bar to 5 bar, respectively. Different reaction mechanisms were used, namely GRI30, DLR, USC/II, Caltech2.3 and ABF. The performance of the CH<sub>2</sub>OxOH as a marker for HRR is assessed in terms of correlation coefficients of their profiles in laminar flames.

The comparison of the obtained correlations of CH<sub>4</sub>/air and CH<sub>4</sub>/O<sub>2</sub> flames shows that in case of air combustion, the HRR can be accurately estimated by the product of CH<sub>2</sub>OxOH for slightly rich flames ( $\Phi = 1.5$ ), whereas the quality of the correlation degrades with increasing equivalence ratio. In contrary, the correlation coefficient increases with higher equivalence ratios in the fuel-rich domain for enhanced oxygen contents in the oxidizer. For pure oxy-fuel combustion, the best correlation is found at an equivalence ratio of approximately  $\Phi = 3.0$ . Elevated pressure leads in all flames to better correlations at lower equivalence ratios compared to standard inlet conditions, whereas preheating induces the opposite trend and expands the valid regime.

A series of CH<sub>4</sub>/air flames were also investigated experimentally in a range of the equivalence ratio between  $1 < \Phi < 2$  at standard inlet conditions. The qualitative CH<sub>2</sub>O (excitation at 355 nm) and OH (excitation at 283 nm) concentration were resolved applying two-dimensional LIF for flames stabilized at a McKenna burner. Comparisons show similar trends for measurements and numerical simulations.

## 1. Introduction

The local heat release rate (HRR) of flames strongly defines their appearance and characteristics, and is a meaningful measure for the chemical time scale in the combustion process. Since there is no possibility for a direct measurement of the HRR available, much effort has been put in previous studies into finding suitable markers for HRR that can be determined experimentally.

Najm et al. [1] investigated different possible markers in order to measure the flame burning rate. They concluded that CH, OH\*, C<sub>2</sub>\* and CH\* are not reliable flame markers for their premixed methane-air V-flames. The chemical pathway of most of the carbon break down follows mainly the route via CH<sub>4</sub> → CH<sub>3</sub> → CH<sub>2</sub>O → HCO → CO → CO<sub>2</sub>, and hence, the aforementioned markers are not directly linked to this route. In contrast, HCO was found to be an excellent marker and correlates very well to the local HRR over a wide range of unsteady curvatures and strain rates. However, the formation of H<sub>2</sub>O and CO<sub>2</sub> is the primary source of the released heat in hydrocarbon flames and HCO only indicates the forward conversion to the final products H<sub>2</sub>O and CO<sub>2</sub>.

The direct experimental measurement of HCO with planar laser-induced fluorescence (PLIF) was demonstrated in the same work [1] where a signal-to-noise ratio (SNR) of the order 2:1 in frame-averaged

images (100 frames) was obtained. Jeffries et al. [2] measured in methane/oxygen ( $\Phi = 1.03$ ) flames at low pressure (5.8 torr) a SNR of approximately 3:1.

Kiefer et al. [3] achieved in single-shot images a SNR between 6:1 and 12:1 in a lean methane/oxygen flame. They extended the work for turbulent premixed methane-air flames and presented useful strategies for HCO-detection [4]. They also recommended restricting the application of HCO PLIF detection to lean or stoichiometric conditions, since larger hydrocarbons will lead to strong interference to the weak HCO signal. Additionally, too high laser pulse energy leads to artificial HCO generated by photolysis of CH<sub>2</sub>O, which restricts to exceed a certain signal level increase by increasing the laser energy.

To overcome those experimental challenges, another approach for HRR detection was introduced by Paul and Najm [5] for a stoichiometric CH<sub>4</sub>/air flame. It is based on the determination of the HRR via the formaldehyde (CH<sub>2</sub>O) and the hydroxyl radical (OH) in order to form the product of both species. This product correlates very well with the formyl (HCO) concentration and hence with the HRR.

The experimental application of this method is widely used because the simultaneous detection of both species is feasible even in turbulent flames by applying LIF. The scope of the present study is to investigate the validity of the HRR marker CH<sub>2</sub>OxOH

\* Corresponding author: Matthias.Sentko@kit.edu  
Proceedings of the European Combustion Meeting 2019

for use in oxygen-enhanced/oxy-fuel and/or fuel-rich premixed flames. In order to identify regimes of applicability for CH<sub>2</sub>OxOH as a valid marker, a parametric study was performed from air to oxy-fuel combustion with variation of equivalence ratio, preheating temperature and pressure using different kinetic schemes. Special focus was set on fuel-rich flames, since the C<sub>2</sub>-pathway of the fuel conversion plays an important role in this domain.

## 2. Numerical Approach

In the present study, the numerical calculations were carried out using the CKReactorFreelyPropagatingFlame program of the ANSYS Chemkin Pro 17.0 package [6]. This program is an advanced development of the PREMIX code originally developed by Kee et al. [7] and solves the 1d, steady state balance equations of species and energy that describe the flame dynamics in a laminar premixed planar flame using implicit finite difference methods. The solver algorithm employed uses a coarse-to-fine grid refinement in order to provide optimal mesh placement. Typically, the calculations start with a grid of about 10-50 points and are assumed to be grid independent at a number of 300-600 points, depending on the complexity of the used chemical scheme. As a measure for the grid independence, normalized criteria with respect to maximal changes in the values and gradients of species between adjacent points are employed (0.05 and 0.07). The freely propagating flame algorithm is used to determine the characteristic flame speed of the gas mixture at the specified pressure and inlet temperature. It automatically adjusts the velocity of incoming fluid to maintain the fluid velocity constant at a point in the flame with a selected temperature.

In the current work, special emphasis was laid on the evolution of species profiles that may resemble the profile of heat release rate. The chemical schemes that were used comprise the relatively simple GRI3.0 reaction mechanism [8] consisting of 53 species and 325 reactions as the reference. With focus on fuel-rich flames, additionally four newer mechanisms with detailed C<sub>2</sub>-pathway chemistry were chosen, ABF [9], DLR [10], USC/II [11] and the CalTech2.3 [12],[13] mechanism, respectively.

The study considers CH<sub>4</sub>/N<sub>2</sub>-O<sub>2</sub>-flames, where the content of O<sub>2</sub> in the oxidizer was changed stepwise from air to pure oxy-fuel conditions. In order to assess the quality of the heat release rate markers for different flame conditions, a broad range of the equivalence ratio of 0.5 < Φ < 3.3 was investigated. Additionally, the inlet temperature of the mixture was varied between 300 K, 473 K and 573 K and pressure between 1 bar, 2 bar and 5 bar. The parameters were varied for each of the chosen mechanisms, which leads to a total number of approx. 4,500 calculated laminar flames.

## 3. Experimental Approach

The fundamentals of laser-induced fluorescence are summarized by A. Eckbreth [14]. The experimental setup is described in detail in [15].

The OH excitation was performed near 283 nm, where Q<sub>1</sub>(7) line of the A-X (1,0) band was used. The fluorescence signal was collected selectively at the A-X (0,0) and (1,1) bands with a band pass filter. The pulse energy was approximately 10 mJ/pulse. PAH fluorescence was separately recorded by detuning the laser wavelength and subtracted subsequently.

The CH<sub>2</sub>O was excited at the strong A-X4<sub>1</sub><sup>0</sup> vibronic band using the 3<sup>rd</sup> harmonic of a Nd:YAG at 355 nm. The mean pulse energy was approximately 170 mJ/pulse. The detection of the fluorescence signal was at 417 nm (FWHM of 60 nm).

The 2d LIF images were recorded with an intensified CDD (12 bit, 1 Mpx). The spatial resolution was approximately 55 x 55 μm in both measurements. The fluctuation of the laser energy was recorded and equalized for each single shot. Finally, mean pictures were averaged out of 280 single shots.

The CH<sub>4</sub>-air flames were stabilized using a McKenna burner. The inlet velocity was set to 6.5 cm/s using Bronkhorst mass flow controllers. A stabilization plate was placed at 150 mm above the burner.

## 4. Determination of the correlation coefficient

In order to assess how strong the association between a species-based marker and the heat release rate, it is necessary to quantify how well the profile of such a marker corresponds to the profile of the heat release rate (HRR) over the entire reaction progress or another equivalent ordinate variable. The result of such an assessment should consider the position of the maximum HRR as well as its profile shape. The strength of the association between species and HRR has been calculated via the Pearson's linear regression coefficient between data on the profiles of both quantities at specified positions of the spatial coordinate, because such data can be measured, too. The Pearson coefficient R between HRR values and the values of an arbitrary marker M is defined as

$$R = \frac{\sum_{i=1}^n (HRR_i - \overline{HRR})(M_i - \overline{M})}{\sqrt{\sum_{i=1}^n (HRR_i - \overline{HRR})^2} \sqrt{\sum_{i=1}^n (M_i - \overline{M})^2}}$$

with  $HRR_i$  and  $M_i$  denoting the  $i^{\text{th}}$  value of a number of HRR values and the corresponding marker quantity;  $\overline{HRR}$  and  $\overline{M}$  stand for the arithmetic mean value of both data series and n for the number of samples in these series.

In order to ensure meaningful values of R as a measure to assess the quality of the marker, a comparable base in terms of the ordinate of the profiles (e.g. the spatial flame coordinate) and its resolution has to be chosen that weights different flame regions equally. Calculation results of the 1D laminar

premixed flame code are obtained on an adaptive grid, having much finer, but problem dependent grid resolution in the main reaction zone. Therefore, the result of just correlating pure calculated quantities would lead to correlation results that are biased due to the local grid resolution. In order to prevent this, 500 values have been sampled equidistantly from a profile domain relevant for heat release (defined as the domain where values of HRR are larger than 10% of its maximum value). As an example, Figure 1 depicts this procedure for an atmospheric CH<sub>4</sub>-air flame for equivalence ratio  $\Phi = 1.67$ , preheat temperature 300 K and 1 bar. The plot shows only every 10<sup>th</sup> sampling point of the HRR and of the product of mole fractions of CH<sub>2</sub>O and OH used as a marker.

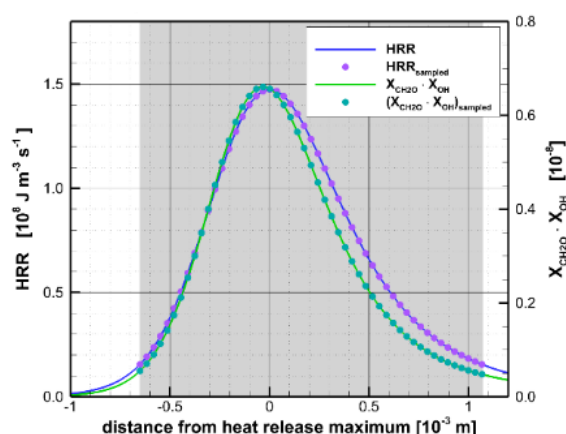


**Figure 1.** Resampled profiles of heat release rate and the product of the mole fractions of CH<sub>2</sub>O and OH as a marker.

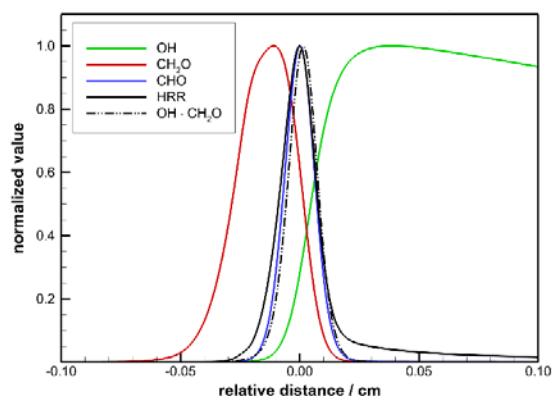


**Figure 2.** Selected species and HRR of a calculated one-dimensional CH<sub>4</sub>/air flame at  $\Phi = 1.0$  (CalTech2.3, 1 bar, 300K).

#### 4. Preliminary Investigations

Species that are detectable by optical diagnostics and used in literature, solely or in combination, as marker species for HRR are OH, CH<sub>2</sub>O and HCO. Therefore, profiles of OH, CH<sub>2</sub>O, HCO, the product CH<sub>2</sub>OxOH and the HRR are exemplary presented normalized in Figure 2 for a stoichiometric CH<sub>4</sub>-air flame at standard inlet conditions, calculated with the Caltech2.3 chemical scheme. With respect to the

species shown, CH<sub>2</sub>O is formed first, whereas the formation of OH starts approximately, where CH<sub>2</sub>O concentration peaks. The product of CH<sub>2</sub>OxOH correlates very well with the HCO concentrations and both adequate with the HRR. However, a slight shift between HRR and HCO or CH<sub>2</sub>OxOH is observed.

Previous investigations in literature are mainly restricted to hydrocarbon/air flames near stoichiometric conditions. In order to give a first impression of the relation between heat release rate and CH<sub>2</sub>OxOH under oxy-fuel conditions a comparison between premixed CH<sub>4</sub>/air and CH<sub>4</sub>/O<sub>2</sub> flames is shown in Figure 3 for different equivalence ratios at standard inlet conditions.

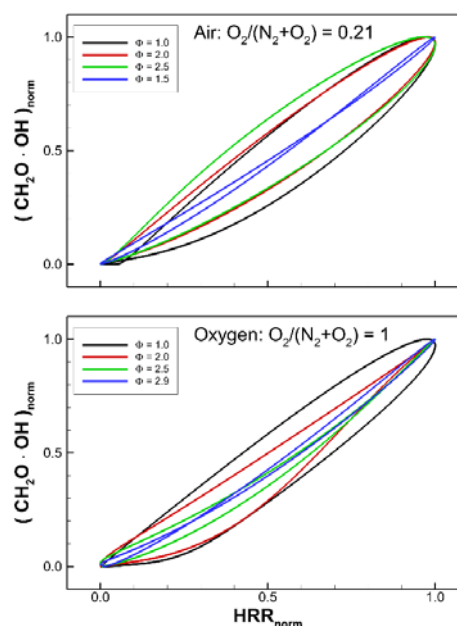


**Figure 3.** Correlation between HRR and CH<sub>2</sub>OxOH, each normalized with their peak-value for CH<sub>4</sub>/air and pure CH<sub>4</sub>/O<sub>2</sub> at selected equivalence ratios (CalTech2.3, 1 bar, 300K).

The shown profiles all fill only a relatively narrow domain near the diagonal of the graph, which is an indication for the general applicability of the marker. Looking into details, it is found that for CH<sub>4</sub>-air flames an almost linear correlation is found for slightly rich flames at an equivalence ratio of  $\Phi = 1.5$ . The correlation quality deteriorates towards stoichiometric and richer flames, which can be assessed by the broadness of the profiles. In contrast, for pure oxy-fuel flames the best correlation is observed for ultra-rich flames ( $\Phi = 2.9$ ) and degrades towards leaner flames.

However, the maximum of the HRR correlates well with the maximum of the marker CH<sub>2</sub>OxOH in all cases.

#### 5. Results and Discussion

In the following section, first the influence of O<sub>2</sub>-content and equivalence ratio on the correlation between CH<sub>2</sub>OxOH and HRR is discussed. Then, the

influence of preheating and pressure are presented and the results of selected reaction mechanism are compared. In the last section, experimental results of rich CH<sub>4</sub>-air flames are shown.

### 5.1. Influence of O<sub>2</sub>-content and equivalence ratio

The normalized product of CH<sub>2</sub>OxOH and HRR are presented in the spatial domain of interest for selected cases in Figure 4. The top row depicts profiles obtained for air combustion and the bottom row shows profiles of oxy-fuel combustion. For both flame types, as the equivalence ratio increases from left ( $\Phi = 1.0$ ) to right ( $\Phi = 2.86$ ), a shift of the relative position of the peak-value of CH<sub>2</sub>OxOH with respect to HRR is observed. In case of stoichiometric mixture and air combustion, the maximum of the HRR is found before the product of CH<sub>2</sub>OxOH while for  $\Phi = 1.5$  an almost perfect overlap is seen, which results finally in the highest correlation coefficient R. A further increase of equivalence ratio leads to profiles where the peak of CH<sub>2</sub>OxOH is found before the one of HRR, which leads to a decrease of the correlation coefficient. A similar trend is found for oxy-fuel combustion, however, the profiles shift towards an overlap at higher equivalence ratios ( $\Phi = 2.9$ ).

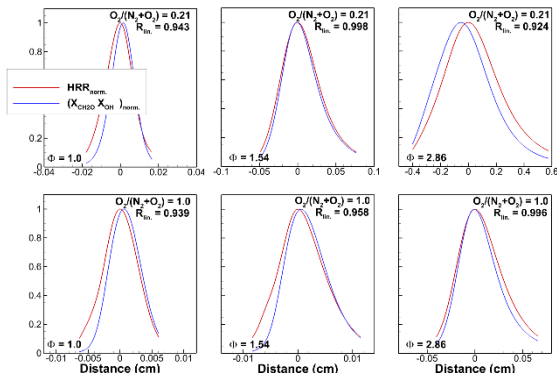


Figure 4. CH<sub>2</sub>OxOH and HRR in spatial domain for selected cases of CH<sub>4</sub>/air- and CH<sub>4</sub>/O<sub>2</sub>-flames (CalTech2.3, 1 bar, 300K).

In order to validate this first visual impression, Pearson's correlation coefficient R is shown in Figure 5. It can be seen that the correlation coefficient exhibits high values ( $R > 0.9$ ) over the whole range examined, which reflects the overall good performance of the marker for HRR. From a comparison of Figure 4 and Figure 5, additionally it is observed that only in flames with correlation coefficients  $R > 0.98$  the marker CH<sub>2</sub>OxOH is able reproduce the shape and position of the HRR profile. For air combustion only small ranges around  $\Phi = 0.5$  and  $\Phi = 1.5$  exhibit such large values of R, while for stoichiometric flames and rich flames with  $\Phi > 2$  the correlation degrades. In contrast, oxygen flames exhibit the worst R for lean flames at  $\Phi \approx 0.65$  while the correlation coefficient increases monotonically until  $\Phi = 3.0$ .

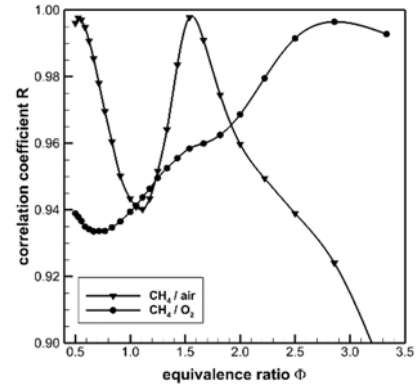


Figure 5. Pearson correlation coefficient of CH<sub>2</sub>OxOH vs. HRR for CH<sub>4</sub>/air and CH<sub>4</sub>/O<sub>2</sub> varying equivalence ratio (CalTech2.3, 1bar, 300K).

### 5.2 Influence of preheating and pressure

Preheating and elevated pressure level have significant influence on the reaction pathway and, thus might have a strong influence on the domain of validity of CH<sub>2</sub>OxOH as a marker for HRR. Figure 6 therefore compares profiles of R varying equivalence ratio for air combustion and for oxy-fuel combustion obtained with preheating and at elevated pressure level. In general, it is found that the principal course of the profiles remains unchanged for all conditions when comparing the different thermo-dynamic conditions: for air combustion, there are two domains of equivalence ratio where high R is found ( $\Phi \approx 0.5$  and  $\Phi \approx 1.5$ ) while low R is obtained at stoichiometric conditions.

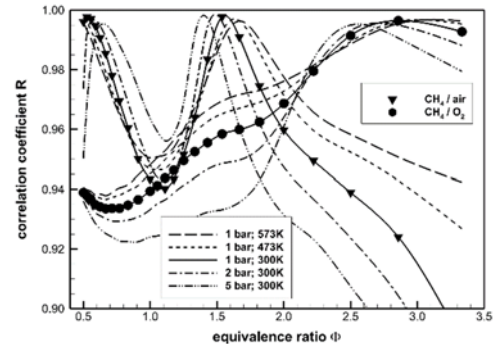


Figure 6. Pearson correlation coefficient of HRR vs. CH<sub>2</sub>OxOH for CH<sub>4</sub>/air and CH<sub>4</sub>/O<sub>2</sub> varying equivalence ratio (CalTech2.3, 1 bar, 300K).

The correlation coefficient R for the complete range of calculated flames is shown as colour map in Figure 7, where additionally the equivalence ratio of the lean maximum correlation coefficient and of the rich minimum for the different thermodynamic conditions is marked with lines.

In case of CH<sub>4</sub>-O<sub>2</sub> flames, the overall monotonic increase of the correlation coefficient with increasing the equivalence ratio remains for both, preheating and elevated pressure. However, similar to CH<sub>4</sub>-air flames, preheating leads to a shift to higher equivalence ratios

and elevated pressure to lower. Near stoichiometric conditions, the trend differs from air combustion: here, elevated pressure leads to a decrease of the correlation coefficient.

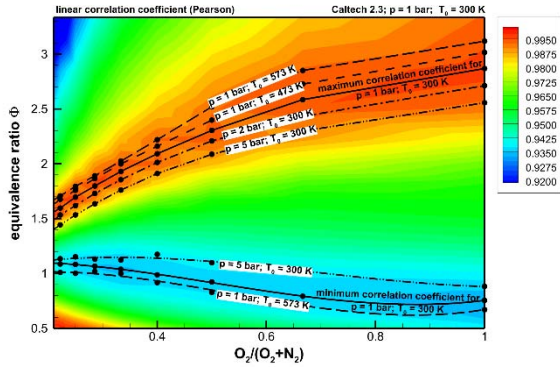


Figure 7. Correlation coefficient depending on equivalence ratio and  $O_2$ -content (Caltech2.3, varying inlet conditions).

### 5.3 Reaction mechanisms

The correlation coefficient map obtained using the USC/II mechanism is presented in Figure 8. In comparison with the results obtained using CalTech2.3 (Figure 7), it is seen that the overall trend is similar. However, the maximum correlation coefficient is found at higher equivalence ratios, while the minimum is found at stoichiometric conditions. The influence of preheating and elevated pressure is the same as described in the previous section.

The equivalence ratio, where the highest correlation coefficient is found, depends on the  $O_2$ -content of the oxidizer and is presented in Figure 9 for different mechanisms at standard conditions. The calculations with the GRI3.0 and CalTech2.3 show an increase of the maximum correlation coefficient from  $\Phi = 1.5$  for air flames to  $\Phi = 2.9$  for pure oxy-fuel flames. The results of both mechanisms are almost superimposable. An overall shift to higher equivalence ratios are found in the calculations with the ABF and USC/II ( $\Phi = 1.7$  to  $\Phi = 3.3$ ). The DLR mechanism shows a good correlation of the  $CH_2OxOH$  with HRR in oxygen-enhance regime highly rich flames. Looking into details, Figure 10 compares the profiles of  $R$  varying equivalence ratio for the set of different mechanisms and air as well as oxygen combustion.

However, the calculated correlation coefficient also differs in quantity for the different used mechanisms that is plotted for  $CH_4$ -air and  $CH_4$ - $O_2$  flames in Figure 10. Especially in case of oxy-fuel combustion, the influence of the reaction scheme on  $R$  is most pronounced. The ABF and USC/II mechanism show lowest correlation coefficient ( $R \approx 0.73$ ) near stoichiometry, while the CalTech2.3 shows highest  $R$ . All mechanisms show an  $R_{max}$  at an equivalence ratio of  $\Phi \approx 3.0$ . A similar trend is for  $CH_4$ -air flames for all mechanisms observed with two  $R_{max}$  at  $\Phi \approx 0.5$  and  $\Phi \approx 1.5$ , respectively.

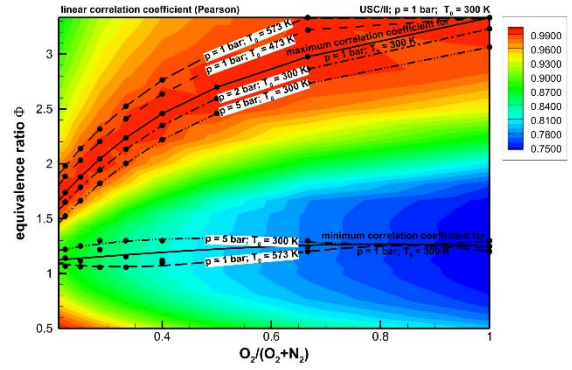


Figure 8. Correlation coefficient depending on equivalence ratio and  $O_2$ -content (USC/II, varying inlet conditions).

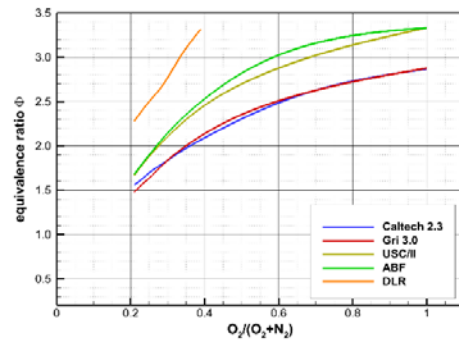


Figure 9. Equivalence ratio with maximum correlation coefficient depending on  $O_2$ -content calculated with different mechanism.

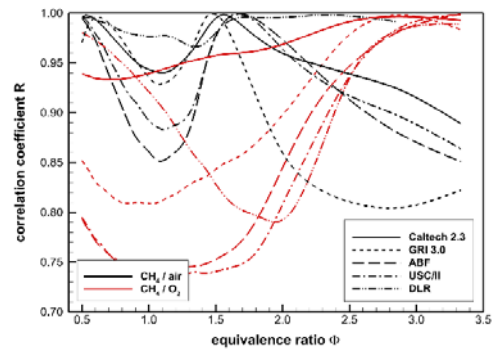
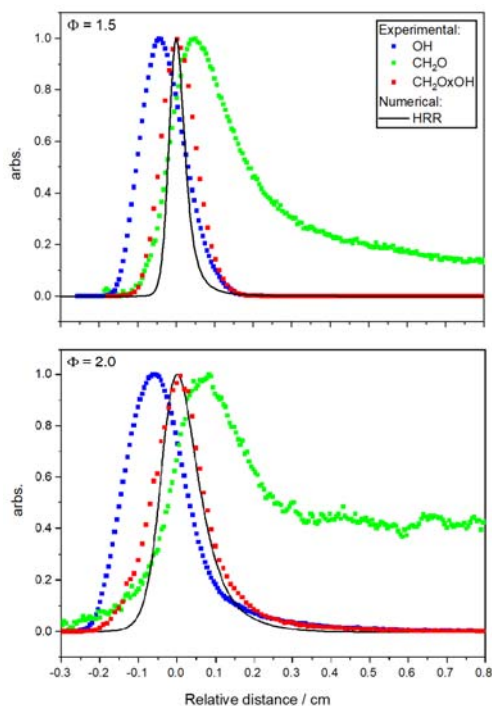


Figure 10. Comparison of the quantity of the correlation coefficient for different mechanism (1bar, 300K).

### 5.4 Experimental Results

The experimental results of the  $OH$ -LIF,  $CH_2O$ -LIF and their product in comparison with numerical simulations are presented for equivalence  $\Phi = 1.5$  and  $\Phi = 2.0$  in Figure 11. As expected, the  $CH_2O$  is formed and consumed within the flame front. Further upstream, the  $OH$ -formation takes place and reaches after its peak value equilibrium concentration. With increasing the equivalence ratio, the flame front broadens in spatial extent. This can be observed in the species profiles, their product  $CH_2OxOH$  as well as the HRR.



**Figure 11. OH- and CH<sub>2</sub>O-LIF, their product in comparison with calculations (CalTech2.3) for an equivalence ratio of  $\Phi = 1.5$  and  $\Phi = 2.0$  (1bar, 300K).**

The experimental results show the same trend as the numerical calculations: with increased equivalence ratio, the HRR marker CH<sub>2</sub>OxOH show better performance in comparison with the numerical results. However, the best agreement is found at a richer equivalence ratio of  $\Phi = 2.0$  compared to the calculations ( $\Phi = 1.5$ ). At leaner conditions, the product of CH<sub>2</sub>OxOH from experimental data show a wider profile than the numerical ones.

### Conclusions

The results show that the HRR of the high temperature oxidation can be reproduced well with the marker CH<sub>2</sub>OxOH. For CH<sub>4</sub>-air flames, the best performance was found for slightly rich conditions at an equivalence ratio of  $\Phi = 1.5$ . Additionally, a second maximum of the correlation coefficient was observed in lean flames ( $\Phi \approx 0.5$ ). In the case of oxy-fuel rich flames, the highest correlation coefficient is found at an equivalence ratio of  $2.5 < \Phi < 3.0$ . In all cases near stoichiometry, a relatively low correlation coefficient was found. An increase of the preheat temperature leads to an expansion of the valid domain, while elevated pressure shifts the domain to slightly lower equivalence ratios and decreases the domain with high correlation coefficients. The experimental results confirm the findings for CH<sub>4</sub>-air flames, with good agreement between measured CH<sub>2</sub>OxOH and calculated HRR for rich flames ( $\Phi \approx 2.0$ ).

### Acknowledgements

The present research work contributes to the Research Field Energy of Helmholtz Association (HGF). The authors would like gratefully to acknowledge the financial support by the German Research Foundation (DFG) for measuring equipment under HFBG programme INST 267/43-1 FUGG and INST 121384/178-1 FUGG.

### References

- [1] H.N. Najm, P.H. Paul, C.J. Mueller, P.S. Wyckoff, *Combust. Flame* 113 (1998) 312–332.
- [2] J.B. Jeffries, D.R. Crosley, I.J. Wysong, G.P. Smith, *Symposium (International) on Combustion* 23 (1991) 1847–1854.
- [3] J. Kiefer, Z.S. Li, T. Seeger, A. Leipertz, M. Aldén, *Proc. Combust. Inst.* 32 (2009) 921–928.
- [4] B. Zhou, J. Kiefer, J. Zetterberg, Z. Li, M. Aldén, *Combust. Flame* 161 (2014) 1566–1574.
- [5] P.H. Paul, H.N. Najm, *Symposium (International) on Combustion* 27 (1998) 43–50.
- [6] ANSYS Chemkin Theory Manual 17.0 (15151), Reaction Design: San Diego, 2015.
- [7] R.J. Kee, F.M. Rupley, J.A. Miller, Report No. SAND 89-8009B, CHEMKIN-II: A Fortran chemical kinetics package for the analysis of gas phase chemical kinetics, Report No. SAND 89-8009B, 1989.
- [8] G.P. Smith, D.M. Golden, M. Frenklach, N.W. Moriarty, B. Eiteneer, M. Goldenberg, C.T. Bowman, R.K. Hanson, S. Song, W.C.J. Gardiner, V.V. Lissianski, Z. Qin, GRI 3.0, 2000, [http://www.me.berkeley.edu/gri\\_mech/](http://www.me.berkeley.edu/gri_mech/).
- [9] J. Appel, H. Bockhorn, M. Frenklach, *Combust. Flame* 121 (2000) 122–136.
- [10] V. Chernov, M.J. Thomson, S.B. Dworkin, N.A. Slavinskaya, U. Riedel, *Combust. Flame* 161 (2014) 592–601.
- [11] H. Wang, X. You, A.V. Joshi, S.G. Davis, A. Laskin, F. Egolfopoulos, C.K. Law, USC Mech Version II. 2007, [http://ignis.usc.edu/USC\\_Mech\\_II.htm](http://ignis.usc.edu/USC_Mech_II.htm).
- [12] K. Narayanaswamy, G. Blanquart, H. Pitsch, *Combust. Flame* 157 (2010) 1879–1898.
- [13] G. Blanquart, *Int. J. Quantum Chem.* 115 (2015) 796–801.
- [14] A.C. Eckbreth, *Laser diagnostics for combustion temperature and species*, CRC Press, Boca Raton, 1996.
- [15] B. Stelzner, F. Hunger, S. Voss, J. Keller, C. Hasse, D. Trimis, *Proc. Combust. Inst.* 34 (2013) 1045–1055.